Space-time Mixing Attention for Video Transformer

Anonymous Author(s)
Affiliation
Address
email

Abstract

This paper is on video recognition using Transformers. Very recent attempts in this area have demonstrated promising results in terms of recognition accuracy, yet they have been also shown to induce, in many cases, significant computational overheads due to the additional modelling of the temporal information. In this work, we propose a Video Transformer model the complexity of which scales linearly with the number of frames in the video sequence and hence induces *no overhead* compared to an image-based Transformer model. To achieve this, our model makes two approximations to the full space-time attention used in Video Transformers: (a) It restricts time attention to a local temporal window and capitalizes on the Transformer's depth to obtain full temporal coverage of the video sequence. (b) It uses efficient space-time mixing to attend *jointly* spatial and temporal locations without inducing any additional cost on top of a spatial-only attention model. We also show how to integrate 2 very lightweight mechanisms for global temporal-only attention which provide additional accuracy improvements at minimal computational cost. We demonstrate that our model produces very high recognition accuracy on the most popular video recognition datasets while at the same time being significantly more efficient than other Video Transformer models. Code will be made available.

1 Introduction

Video recognition – in analogy to image recognition – refers to the problem of recognizing events of interest in video sequences such as human activities. Following the tremendous success of Transformers in sequential data, specifically in Natural Language Processing (NLP) [37, 5], Vision Transformers were very recently shown to outperform CNNs for image recognition too [45, 12, 33], signaling a paradigm shift on how visual understanding models should be constructed. In light of this, in this paper, we propose a Video Transformer model as an appealing and promising solution for improving the accuracy of video recognition models.

A direct, natural extension of Vision Transformers to the spatio-temporal domain is to perform the self-attention *jointly* across all S spatial locations and T temporal locations. Full space-time attention though has complexity $O(T^2S^2)$ making such a model computationally heavy and, hence, impractical even when compared with the 3D-based convolutional models. As such, our aim is to exploit the temporal information present in video streams while minimizing the computational burden within the Transformer framework for efficient video recognition.

A baseline solution to this problem is to consider spatial-only attention followed by temporal averaging, which has complexity $O(TS^2)$. Similar attempts to reduce the cost of full space-time attention have been recently proposed in [3, 1]. These methods have demonstrated promising results in terms of video recognition accuracy, yet they have been also shown to induce, in most of the cases, significant computational overheads compared to the baseline (spatial-only) method due to the additional modelling of the temporal information.

Submitted to 35th Conference on Neural Information Processing Systems (NeurIPS 2021). Do not distribute.

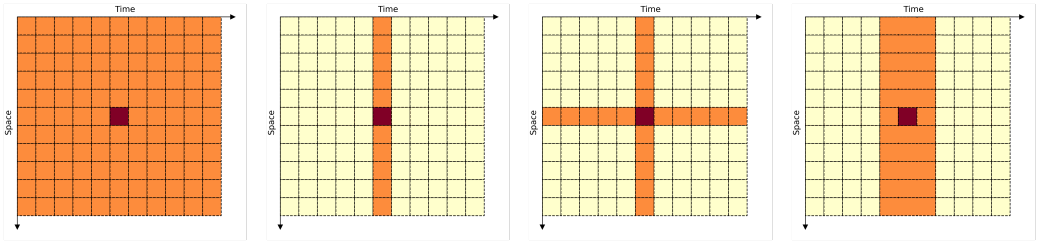

(a) Full space-time attention: $O(T^2S^2)$ (b) Spatial-only attention: $O(TS^2)$ (c) TimeSformer [3]: $O(T^2S + TS^2)$ (d) Ours: $O(TS^2)$

Figure 1: Different approaches to space-time self-attention for video recognition. In all cases, the key locations that the query vector, located at the center of the grid in red, attends are shown in orange. Unlike prior work, our key vector is constructed by mixing information from tokens located at the same spatial location within a local temporal window. Our method then performs self-attention with these tokens. Note that our mechanism allows for an efficient approximation of local space-time attention at no extra cost.

Our main contribution in this paper is a Video Transformer model that has complexity $O(TS^2)$ and, hence, is as efficient as the baseline model, yet, as our results show, it outperforms recently/concurrently proposed work [3, 1] in terms of efficiency (*i.e.* accuracy/FLOP) by significant margins. To achieve this our model makes two approximations to the full space-time attention used in Video Transformers: (a) It restricts time attention to a local temporal window and capitalizes on the Transformer's depth to obtain full temporal coverage of the video sequence. (b) It uses efficient space-time mixing to attend *jointly* spatial and temporal locations without inducing any additional cost on top of a spatial-only attention model. Fig. 1 shows the proposed approximation to space-time attention. We also show how to integrate two very lightweight mechanisms for global temporal-only attention, which provide additional accuracy improvements at minimal computational cost. We demonstrate that our model is surprisingly effective in terms of capturing long-term dependencies and producing very high recognition accuracy on the most popular video recognition datasets, including Something-Something-v2 [16], Kinetics [4] and Epic Kitchens [8], while at the same time being significantly more efficient than other Video Transformer models.

2 Related work

Video recognition: Standard solutions are based on CNNs and can be broadly classified into two categories: 2D- and 3D-based approaches. 2D-based approaches process each frame independently to extract frame-based features which are then aggregated temporally with some sort of temporal modeling (e.g. temporal averaging) performed at the end of the network [40, 25, 26]. The works of [25, 26] use the "shift trick" [42] to have some temporal modeling at a layer level. 3D-based approaches [4, 15, 34] are considered the current state-of-the-art as they can typically learn stronger temporal models via 3D convolutions. However, they also incur higher computational and memory costs. To alleviate this, a large body of works attempt to improve their efficiency via spatial and/or temporal factorization [36, 35, 14].

CNN vs ViT: Historically, video recognition approaches tend to mimic the architectures used for image classification (e.g. from AlexNet [22] to [19] or from ResNet [17] and ResNeXt [44] to [15]). After revolutionizing NLP [37, 30], very recently, Transformer-based architectures showed promising results on large scale image classification too [12]. While self-attention and attention were previously used in conjunction with CNNs at a layer or block level [6, 46, 31], the Vision Transformer (ViT) of Dosovitskiy et al. [12] is the first convolution-free, Transformer-based architecture that achieves state-of-the-art on ImageNet [10].

Video Transformer: Recently/concurrently with our work, vision transformer architectures, derived from [12], were used for video recognition [3, 1], too. Because performing full space-time attention is computationally prohibitive (*i.e.* $O(T^2S^2)$), their main focus is on reducing this via temporal and spatial factorization. In TimeSformer [3], the authors propose applying spatial and temporal attention in an alternating manner reducing the complexity to $O(T^2S + TS^2)$. In a similar fashion, ViViT [1] explores several avenues for space-time factorization. In addition, they also proposed to adapt the

patch embedding process from [12] to 3D (*i.e.* video) data. Our work proposes a completely different approximation to full space-time attention that is also efficient. To this end, we firstly restrict full space-time attention to a local temporal window which is reminiscent of [2] but applied here to space-time attention and video recognition. Secondly, we define a local joint space-time attention which we show that can be implemented efficiently via the "shift trick" [42].

3 Method

Video Transformer: We are given a video clip $\mathbf{X} \in \mathbb{R}^{T \times H \times W \times C}$ ($C = 3$). Following ViT [12], each frame is divided into $K \times K$ non-overlapping patches which are then mapped into visual tokens using a linear embedding layer $\mathbf{E} \in \mathbb{R}^{3K^2 \times d}$. Since self-attention is permutation invariant, in order to preserve the information regarding the location of each patch within space and time we also learn two positional embeddings, one for space: $\mathbf{p}_s \in \mathbb{R}^{1 \times S \times d}$ and one for time: $\mathbf{p}_t \in \mathbb{R}^{T \times 1 \times d}$. These are then added to the initial visual tokens. Finally, the token sequence is processed by L Transformer layers.

The visual token at layer l, spatial location s and temporal location t is denoted as:

$$\mathbf{z}^l_{s,t} \in \mathbb{R}^d, \quad l = 0, \ldots, L-1, \;\; s = 0, \ldots, S-1, \;\; t = 0, \ldots, T-1. \tag{1}$$

In addition to the ST visual tokens extracted from the video, a special classification token $\mathbf{z}^l_{cls} \in \mathbb{R}^d$ is prepended to the token sequence [11]. The $l-$th Transformer layer processes the visual tokens $\mathbf{Z}^l \in \mathbb{R}^{(ST+1) \times d}$ of the previous layer using a series of Multi-head Self-Attention (MSA), Layer Normalization (LN), and MLP ($\mathbb{R}^d \rightarrow \mathbb{R}^{4d} \rightarrow \mathbb{R}^d$) layers as follows:

$$\mathbf{Y}^l = \text{MSA}(\text{LN}(\mathbf{Z}^{l-1})) + \mathbf{Z}^{l-1}, \tag{2}$$

$$\mathbf{Z}^{l+1} = \text{MLP}(\text{LN}(\mathbf{Y}^l)) + \mathbf{Y}^l. \tag{3}$$

The main computation of a single full space-time Self-Attention (SA) head boils down to calculating:

$$\mathbf{y}^l_{s,t} = \sum_{t'=0}^{T-1} \sum_{s'=0}^{S-1} \text{Softmax}\{(\mathbf{q}^l_{s,t} \cdot \mathbf{k}^l_{s',t'})/\sqrt{d_h}\}\mathbf{v}^l_{s',t'}, \; \left\{ \begin{smallmatrix} s=0,\ldots,S-1 \\ t=0,\ldots,T-1 \end{smallmatrix} \right\} \tag{4}$$

where $\mathbf{q}^l_{s,t}, \mathbf{k}^l_{s,t}, \mathbf{v}^l_{s,t} \in \mathbb{R}^{d_h}$ are the query, key, and value vectors computed from $\mathbf{z}^l_{s,t}$ (after LN) using embedding matrices $\mathbf{W_q}, \mathbf{W_k}, \mathbf{W_v} \in \mathbb{R}^{d \times d_h}$. Finally, the output of the h heads is concatenated and projected using embedding matrix $\mathbf{W_h} \in \mathbb{R}^{hd_h \times d}$.

The complexity of the full model is: $O(3hTSdd_h)$ (qkv projections) $+O(2hT^2S^2d_h)$ (MSA for h attention heads) $+O(TS(hd_h)d)$ (multi-head projection) $+O(4TSd^2)$ (MLP). From these terms, our goal is to reduce the cost $O(2T^2S^2d_h)$ (for a single attention head) of the full space-time attention which is the dominant term. For clarity, from now on, we will drop constant terms and d_h to report complexity unless necessary. Hence, the complexity of the full space-time attention is $O(T^2S^2)$.

Our baseline is a model that performs a simple approximation to the full space-time attention by applying, at each Transformer layer, spatial-only attention:

$$\mathbf{y}^l_{s,t} = \sum_{s'=0}^{S-1} \text{Softmax}\{(\mathbf{q}^l_{s,t} \cdot \mathbf{k}^l_{s',t})/\sqrt{d_h}\}\mathbf{v}^l_{s',t}, \; \left\{ \begin{smallmatrix} s=0,\ldots,S-1 \\ t=0,\ldots,T-1 \end{smallmatrix} \right\} \tag{5}$$

the complexity of which is $O(TS^2)$. Notably, the complexity of the proposed space-time mixing attention is also $O(TS^2)$. Following spatial-only attention, simple temporal averaging is performed on the class tokens $\mathbf{z}_{final} = \frac{1}{T}\sum_t \mathbf{z}^{L-1}_{t,cls}$ to obtain a single feature that is fed to the linear classifier.

Recent work by [3, 1] has focused on reducing the cost $O(T^2S^2)$ of the full space-time attention of Eq. 4. Bertasius et al. [3] proposed the factorised attention:

$$\begin{aligned} \tilde{\mathbf{y}}^l_{s,t} &= \sum_{t'=0}^{T-1} \text{Softmax}\{(\mathbf{q}^l_{s,t} \cdot \mathbf{k}^l_{s,t'})/\sqrt{d_h}\}\mathbf{v}^l_{s,t'}, \\ \mathbf{y}^l_{s,t} &= \sum_{s'=0}^{S-1} \text{Softmax}\{\tilde{\mathbf{q}}^l_{s,t} \cdot \tilde{\mathbf{k}}^l_{s',t})/\sqrt{d_h}\}\tilde{\mathbf{v}}^l_{s',t}, \end{aligned} \quad \begin{Bmatrix} s = 0, \ldots, S-1 \\ t = 0, \ldots, T-1 \end{Bmatrix}, \tag{6}$$

where $\tilde{\mathbf{q}}^l_{s,t}, \tilde{\mathbf{k}}^l_{s',t} \tilde{\mathbf{v}}^l_{s',t}$ are new query, key and value vectors calculated from $\tilde{\mathbf{y}}^l_{s,t}$ [1]. The above model reduces complexity to $O(T^2S + TS^2)$. However, temporal attention is performed for a fixed spatial location which is ineffective when there is camera or object motion and there is spatial misalignment between frames.

The work of [1] is concurrent to ours and proposes the following approximation: L_s Transformer layers perform spatial-only attention as in Eq. 5 (each with complexity $O(S^2)$). Following this, there are L_t Transformer layers performing temporal-only attention on the class tokens $\mathbf{z}^{L_s}_t$. The complexity of the temporal-only attention is, in general, $O(T^2)$.

Our model aims to better approximate the full space-time self-attention (SA) of Eq. 4 while keeping complexity to $O(TS^2)$, i.e. inducing no further complexity to a spatial-only model.

To achieve this, we make a first approximation to perform full space-time attention but restricted to a local temporal window $[-t_w, t_w]$:

$$\mathbf{y}^l_{s,t} = \sum_{t'=t-t_w}^{t+t_w} \sum_{s'=0}^{S-1} \text{Softmax}\{(\mathbf{q}^l_{s,t} \cdot \mathbf{k}^l_{s',t'})/\sqrt{d_h}\}\mathbf{v}^l_{s',t'} = \sum_{t'=t-t_w}^{t+t_w} \mathbf{V}^l_{t'}\mathbf{a}^l_{t'}, \ \left\{ \begin{smallmatrix} s=0,\ldots,S-1 \\ t=0,\ldots,T-1 \end{smallmatrix} \right\} \tag{7}$$

where $\mathbf{V}^l_{t'} = [\mathbf{v}^l_{0,t'}; \mathbf{v}^l_{1,t'}; \ldots; \mathbf{v}^l_{S-1,t'}] \in \mathbb{R}^{d_h \times S}$ and $\mathbf{a}^l_{t'} = [a^l_{0,t'}, a^l_{1,t'}, \ldots, a^l_{S-1,t'}] \in \mathbb{R}^S$ is the vector with the corresponding attention weights. Eq. 7 shows that, for a single Transformer layer, $\mathbf{y}^l_{s,t}$ is a spatio-temporal combination of the visual tokens in the local window $[-t_w, t_w]$. It follows that, after k Transformer layers, $\mathbf{y}^{l+k}_{s,t}$ will be a spatio-temporal combination of the visual tokens in the local window $[-kt_w, kt_w]$ which in turn conveniently allows to perform spatio-temporal attention over the whole clip. For example, for $t_w = 1$ and $k = 4$, the local window becomes $[-4, 4]$ which spans the whole video clip for the typical case $T = 8$.

The complexity of the local self-attention of Eq. 7 is $O((2t_w + 1)TS^2)$. To reduce this even further, we make a second approximation on top of the first one as follows: the attention between spatial locations s and s' according to the model of Eq. 7 is:

$$\sum_{t'=t-t_w}^{t+t_w} \text{Softmax}\{(\mathbf{q}^l_{s,t} \cdot \mathbf{k}^l_{s',t'})/\sqrt{d_h}\}\mathbf{v}^l_{s',t'}, \tag{8}$$

i.e. it requires the calculation of $2t_w + 1$ attentions, one per temporal location over $[-t_w, t_w]$. Instead, we propose to calculate a single attention over $[-t_w, t_w]$ which can be achieved by $\mathbf{q}^l_{s,t}$ attending $\mathbf{k}^l_{s',-t_w:t_w} \triangleq [\mathbf{k}^l_{s',t-t_w}; \ldots; \mathbf{k}^l_{s',t+t_w}] \in \mathbb{R}^{(2t_w+1)d_h}$. Note that to match the dimensions of $\mathbf{q}^l_{s,t}$ and $\mathbf{k}^l_{s',-t_w:t_w}$ a further projection of $\mathbf{k}^l_{s',-t_w:t_w}$ to $\mathbb{R}^{d_h}$ is normally required which has complexity $O((2t_w + 1)d_h^2)$ and hence compromises the goal of an efficient implementation. To alleviate this we use the "shift trick" [42, 25] which allows to perform both zero-cost dimensionality reduction, space-time mixing and attention (between $\mathbf{q}^l_{s,t}$ and $\mathbf{k}^l_{s',-t_w:t_w}$) in $O(d_h)$. In particular, each $t' \in [-t_w, t_w]$ is assigned $d^{t'}_h$ channels from d_h (i.e. $\sum_{t'} d^{t'}_h = d_h$). Let $\mathbf{k}^l_{s',t'}(d^{t'}_h) \in \mathbb{R}^{d^{t'}_h}$ denote the operator for indexing the $d^{t'}_h$ channels from $\mathbf{k}^l_{s',t'}$. Then, a new key vector is constructed as:

$$\tilde{\mathbf{k}}^l_{s',-t_w:t_w} \triangleq [\mathbf{k}^l_{s',t-t_w}(d^{t-t_w}_h), \ldots, \mathbf{k}^l_{s',t+t_w}(d^{t+t_w}_h)] \in \mathbb{R}^{d_h}. \tag{9}$$

Fig. 2 shows how the key vector $\tilde{\mathbf{k}}^l_{s',-t_w:t_w}$ is constructed. In a similar way, we also construct a new value vector $\tilde{\mathbf{v}}^l_{s',-t_w:t_w}$. Finally, the proposed approximation to the full space-time attention is given by:

$$\mathbf{y}^{l_s}_{s,t} = \sum_{s'=0}^{S-1} \text{Softmax}\{(\mathbf{q}^{l_s}_{s,t} \cdot \tilde{\mathbf{k}}^l_{s',-t_w:t_w}/\sqrt{d_h}\}\tilde{\mathbf{v}}^l_{s',-t_w:t_w}, \ \left\{ \begin{smallmatrix} s=0,\ldots,S-1 \\ t=0,\ldots,T-1 \end{smallmatrix} \right\}. \tag{10}$$

This has the complexity of a spatial-only attention ($O(TS^2)$) and hence it is more efficient than previously proposed video transformers [3, 1]. Our model also provides a better approximation to the full space-time attention and as shown by our results it significantly outperforms [3, 1].

[1] More precisely, Eq. 6 holds for $h = 1$ heads. For $h > 1$, the different heads $\tilde{\mathbf{y}}^{l,h}_{s,t}$ are concatenated and projected to produce $\tilde{\mathbf{y}}^l_{s,t}$.

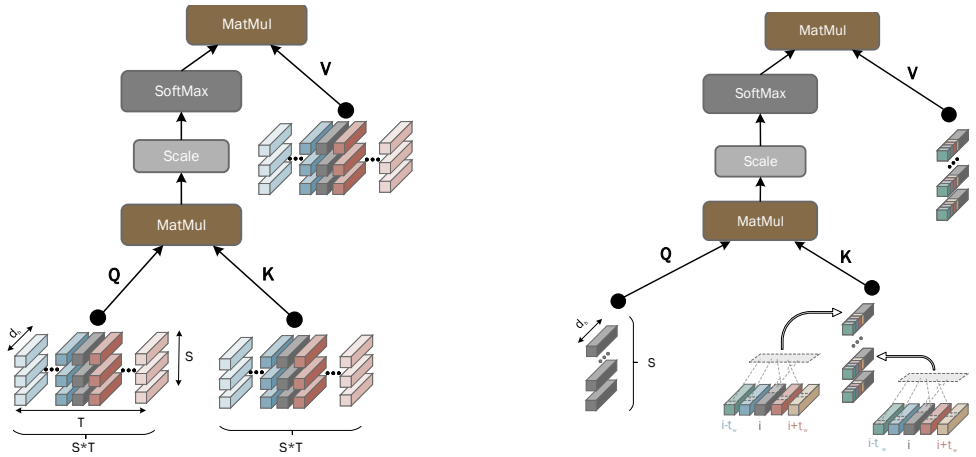

(a) Full Spatio-temporal attention.

(b) Ours.

Figure 2: Detailed self-attention computation graph for (a) full space-time attention and (b) the proposed space-time mixing approximation. Notice that in our case only S tokens participate instead of ST. The temporal information is aggregated by indexing channels from adjacent frames. Tokens of identical colors share the same temporal index.

Temporal Attention aggregation: The final set of the class tokens $\mathbf{z}_{t,cls}^{L-1}, 0 \leq t \leq L-1$ are used to generate the predictions. To this end, we propose to consider the following options: (a) simple temporal averaging $\mathbf{z}_{final} = \frac{1}{T}\sum_t \mathbf{z}_{t,cls}^{L-1}$ as in the case of our baseline. (b) An obvious limitation of temporal averaging is that the output is treated purely as an ensemble of per-frame features and, hence, completely ignores the temporal ordering between them. To address this, we propose to use a lightweight Temporal Attention (TA) mechanism that will attend to the T classification tokens. In particular a $\mathbf{z}_{final}$ token attends the sequence $[\mathbf{z}_{0,cls}^{L-1}, \ldots, \mathbf{z}_{T-1,cls}^{L-1}]$ using a temporal Transformer layer and then fed as input to the classifier. This is akin to the (concurrent) work of [1] with the difference being that in our model we found that a single TA layer suffices whereas [1] uses L_t. A consequence of this is that the complexity of our layer is $O(T)$ vs $O(2(L_t-1)T^2+T)$ of [1].

Summary token: As an alternative to TA, herein, we also propose a simple lightweight mechanism for information exchange between different frames at intermediate layers of the network. Given the set of tokens for each frame t, $\mathbf{Z}_t^{l-1} \in \mathbb{R}^{(S+1)\times d_h}$ (constructed by concatenating all tokens $\mathbf{z}_{s,t}^{l-1}, s = 0, \ldots, S$), we compute a new set of R tokens $\mathbf{Z}_{r,t}^{l} = \phi(\mathbf{Z}_t^{l-1}) \in \mathbb{R}^{R\times d_h}$ which summarize the frame information and hence are named "Summary" tokens. These are then, appended to the visual tokens of all frames to calculate the keys and values so that the query vectors attend the original keys plus the Summary tokens. Herein, we explore the case that $\phi(.)$ performs simple spatial averaging $\mathbf{z}_{0,t}^{l} = \frac{1}{S}\sum_s \mathbf{z}_{s,t}^{l}$ over the tokens of each frame ($R = 1$ for this case) while other functions are considered in the supplementary material. Note that, for $R = 1$, the extra cost that the Summary token induces is $O(TS)$.

X-ViT: We call the Video Transformer based on the proposed (a) space-time mixing attention and (b) lightweight global temporal attention (or summary token) as **X-ViT**.

4 Results

4.1 Experimental setup

Datasets: We train and evaluate the proposed models on the following datasets (all datasets are publicly available for research purposes):

Kinetics-400 and 600: The Kinetics [20] dataset consists of short clips (typically 10 sec long) sampled from YouTube labeled using 400 and 600 classes, respectively. Due to the removal of certain videos from YouTube, the version of the dataset used in this paper consists of approximately 261k clips for Kinetics-400. Note, that this amounts are lower than the original version of the datasets and thus will represent a negative performance bias when compared with prior works.

Something-Something-v2 (SSv2): The SSv2 [16] dataset consists of 220,487 short videos, with a length between 2 and 6 seconds that picture humans performing pre-defined basic actions with everyday objects. Since the objects and backgrounds in the videos are consistent across different action classes, this dataset tends to require stronger temporal modeling. Due to this, we conducted most of our ablation studies on SSv2 to better analyze the importance of the proposed components.

Epic Kitchens-100 (Epic-100): is an egocentric large scale action recognition dataset consisting of more than 90,000 action segments that span across 100 hours of recordings in native environments, capturing daily activities [9]. The dataset is labeled using 97 verb classes and 300 noun classes. The evaluation results are reported using the standard action recognition protocol: the network predicts the "verb" and the "noun" using two heads. The predictions are then merged to construct an "action" which is used to report the accuracy.

Training details: All models, unless otherwise stated, were trained using the following scheduler and training procedure: specifically, our models were trained using SGD with momentum (0.9) and a cosine scheduler [27] (with linear warmup) for 35 epochs on SSv2, 50 on Epic-100 and 30 on Kinetics. The base learning rate, set at a batch size of 128, was 0.05 (0.03 for Kinetics). To prevent over-fitting we made use of the following augmentation techniques: random scaling (0.9$\times$ to 1.3$\times$) and cropping, random flipping (with probability of 0.5; not for SSv2) and autoaugment [7]. In addition, for SSv2 and Epic-100 we also applied random erasing (probability=0.5, min. area=0.02, max. area=1/3, min. aspect=0.3) [48] and label smoothing (λ = 0.3) [32] while, for Kinetics, we used mixup [47] ($\alpha = 0.4$).

The backbone models closely follow the ViT architecture Dosovitskiy et al. [12]. Most of the experiments were performed using the ViT-B/16 variant ($L = 12$, $h = 12$, $d = 768$, $K = 16$), where L represents the number of transformer layers, h the number of heads, d the embedding dimension and K the patch size. We initialized our models from a pretrained ImageNet-21k [10] ViT model. The spatial positional encoding $\mathbf{p}_s$ was initialized from the pretrained 2D model and the temporal one, $\mathbf{p}_t$, with zeros so that it does not have a great impact on the tokens early on during training. The models were trained on 8 V100 GPUs using PyTorch [28].

Testing details: Unless otherwise stated, we used ViT-B/16 and $T = 8$ frames. We mostly used Temporal Attention (TA) for temporal aggregation. We report accuracy results for 1×3 views (1 temporal clip and 3 spatial crops) departing from the common approach of using up to 10×3 views [25, 15]. The 1×3 views setting was also used in Bertasius et al. [3]. To measure the variation between runs, we trained one of the 8–frame models 5 times. The results varied by $\pm 0.4\%$.

4.2 Ablation studies

Throughout this section we study the effect of varying certain design choices and different components of our method. Because SSv2 tends to require a more fine-grained temporal modeling, unless otherwise specified, all results reported, in this subsection, are on the SSv2.

Effect of local window size: Table 1 shows the accuracy of our model by varying the local window size $[-t_w, t_w]$ used in the proposed space-time mixing attention. Firstly, we observe that the proposed model is significantly superior to our baseline ($t_w = 0$) which uses spatial-only attention. Secondly, a window of $t_w = 1$ produces the best results. This shows that more gradual increase of the effective window size that is attended is more beneficial compared to more aggressive ones, i.e. the case where $t_w = 2$. A performance degradation for the case $t_w = 2$ could be attributed to boundary effects (handled by filling with zeros) which are aggravated as t_w increases. Based on these results, we chose to use $t_w = 1$ for the models reported hereafter.

Table 1: Effect of local window size. To isolate its effect from that of temporal aggregation, the models were trained using temporal averaging. Note, that *(Bo.)* indicates that only features from the boundaries of the local window were used, ignoring the intermediary ones.

Variant	Top-1	Top-5
$t_w = 0$	44.2	71.4
$t_w = 1$	**61.6**	**87.8**
$t_w = 2$	59.7	86.4
$t_w = 2$ (Bo.)	59.6	86.2

Effect of SA position: We explored which layers should the proposed space-time mixing attention operation be applied to *within the Transformer*. Specifically, we explored the following variants: Applying it to the first $L/2$ layers, to the last $L/2$ layers, to every odd indexed layer and finally, to all layers. As the results from Table 2a show, the exact layers within the network that self-attention is

Table 2: Effect of (a) proposed SA position, (b) temporal aggregation and number of Temporal Attention (TA) layers, (c) space-time mixing qkv vectors and (d) amount of mixed channels on SSv2.

(a) Effect of applying the proposed SA to certain layers.

Transform. layers	Top-1	Top-5
1st half	60.7	86.5
2nd half	60.6	86.3
Half (odd. pos)	60.3	86.4
All	61.6	87.8

(b) Effect of number of TA layers. 0 corresponds to temporal averaging.

#. TA layers	Top-1	Top-5
0 (temp. avg.)	61.6	87.8
1	**63.4**	**89.6**
2	63.4	89.6
3	63.4	89.6

(c) Effect of space-time mixing. x denotes the input token before qkv projection. Query produces equivalent results with key and thus omitted.

x	key	value	Top-1	Top-5
✗	✗	✗	55.6	83.5
✓	✗	✗	62.1	88.9
✗	✓	✗	62.1	88.9
✗	✗	✓	61.5	88.7
✗	✓	✓	**63.4**	**89.6**

(d) Effect of amount of mixed channels. * uses temp. avg. aggregation.

0%*	0%	25%	50%	100%
44.2	55.6	63.3	**63.4**	60.7

Table 3: Comparison between TA and Summary token on SSv2 (left) and Kinetics-400 (right).

Summary	TA	Top-1	Top-5
✗	✗	61.6	87.8
✓	✗	62.9	89.2
✓	✓	62.5	89.1
✗	✓	63.4	89.6

Summary	TA	Top-1	Top-5
✗	✗	77.8	93.7
✓	✗	78.7	93.7
✓	✓	78.0	93.2
✗	✓	78.5	93.7

applied to do not matter; what matters is the number of layers it is applied to. We attribute this result to the increased temporal receptive field and cross-frame interactions.

Effect of temporal aggregation: Herein, we compare the two methods used for temporal aggregation: simple temporal averaging [39] and the proposed Temporal Attention (TA) mechanism. Given that our model already incorporates temporal information through the proposed space-time attention, we also explored how many TA layers are needed. As shown in Table 2b replacing temporal averaging with one TA layer improves the Top-1 accuracy from 61.6% to 63.4%. Increasing the number of layers further yields no additional benefits. We also report the accuracy of spatial-only attention plus TA aggregation. In the absence of the proposed space-time mixing attention, the TA layer alone is unable to compensate, scoring only 55.6% as shown in Table 2d. This highlights the need of having both components in our final model. For the next two ablation studies, we therefore used 1 TA layer.

Effect of space-time mixing qkv vectors: Paramount to our work is the proposed space-time mixing attention of Eq. 10 which is implemented by constructing $\tilde{\mathbf{k}}^l_{s',-t_w:t_w}$ and $\tilde{\mathbf{v}}^l_{s',-t_w:t_w}$ efficiently via channel indexing (see Eq. 9). Space-time mixing though can be applied in several different ways in the model. For completeness, herein, we study the effect of space-time mixing to various combinations for the key, value and to the input token prior to qkv projection. As shown in Table 2c, the combination corresponding to our model (*i.e.* space-time mixing applied to the key and value) significantly outperforms all other variants by up to 2%. This result is important as it confirms that our model, derived from the proposed approximation to the local space-time attention, gives the best results when compared to other non-well motivated variants.

Table 4: Effect of number of tokens on SSv2.

Variant	Top-1	Top-5	FLOPs ($\times 10^9$)
ViT-B/32	59.8	87.4	95
ViT-L/32	61.0	88.3	327
ViT-B/16	**63.4**	89.6	425

Effect of amount of space-time mixing: We define as ρd_h the total number of channels imported from the adjacent frames in the local temporal window $[-t_w, t_w]$ (*i.e.* $\sum_{t'=-t_w, t\neq 0}^{t_w} d_h^{t'} = \rho d_h$) when constructing $\tilde{\mathbf{k}}^l_{s',-t_w:t_w}$ (see Section 3). Herein, we study the effect of ρ on the model's accuracy. As

the results from Table 2d show, the optimal ρ is between 25% and 50%. Increasing ρ to 100% (*i.e.* all channels are coming from adjacent frames) unsurprisingly degrades the performance as it excludes the case $t' = t$ when performing the self-attention.

Effect of Summary token: Herein, we compare Temporal Attention with Summary token on SSv2 and Kinetics-400. We used both datasets for this case as they require different type of understanding: fine-grained temporal (SSv2) and spatial content (K400). From Table 3, we conclude that the Summary token compares favorable on Kinetics-400 but not on SSv2 showing that is more useful in terms of capturing spatial information. Since the improvement is small, we conclude that 1 TA layer is the best global attention-based mechanism for improving the accuracy of our method adding also negligible computational cost.

Effect of the number of input frames: Herein we evaluate the impact of increasing the number of input frames T from 8 to 16 and 32. We note that, for our method, this change results in a linear increase in complexity. As the results from Table 6 show, increasing the number of frames from 8 to 16 offers a 1.8% boost in Top-1 accuracy on SSv2. Moreover, increasing the number of frames to 32 improves the performance by a further 0.2%, offering diminishing returns. Similar behavior can be observed on Kinetics and Epic-100 in Tables 5 and 7.

Effect of number of tokens: Herein, we vary the number of input tokens by changing the patch size K. As the results from Table 4 show, even when the number of tokens decreases significantly (ViT-B/32) our approach is still able to produce models that achieve satisfactory accuracy. The benefit of that is having a model which is significantly more efficient.

Latency and throughput considerations: While the channel shifting operation used by the proposed space-time mixing attention is zero-FLOP, there is still a small cost associated with memory movement operations. In order to ascertain that the induced cost does not introduce noticeable performance degradation, we benchmarked a Vit-B/16 (8$\times$ frames) model using spatial-only attention and the proposed one on 8 V100 GPUs and a batch size of 128. A model without our space-time attention has a throughput of 312 frames/second while our model has 304 frames/second.

Table 5: Comparison with state-of-the-art on the Kinetics-400. $T\times$ is the number of frames used by our method.

Method	Top-1	Top-5	Views	FLOPs ($\times 10^9$)
bLVNet [13]	73.5	91.2	3×3	840
STM [18]	73.7	91.6	-	-
TEA [24]	76.1	92.5	10×3	2,100
TSM R50 [25]	74.7	-	10×3	650
I3D NL [41]	77.7	93.3	10×3	10,800
CorrNet-101 [38]	79.2	-	10×3	6,700
ip-CSN-152 [36]	79.2	93.8	10×3	3,270
LGD-3D R101 [29]	79.4	94.4	-	-
SlowFast 8$\times$8 R101+NL [15]	78.7	93.5	10×3	3,480
SlowFast 16$\times$8 R101+NL [15]	79.8	93.9	10×3	7,020
X3D-XXL [14]	80.4	94.6	10×3	5,823
TimeSformer-L [3]	**80.7**	94.7	1×3	7,140
ViViT-L/16x2 [3]	80.6	94.7	4×3	17,352
X-ViT (8$\times$) (Ours)	78.5	93.7	1×3	425
X-ViT (16$\times$) (Ours)	80.2	**94.7**	1×3	850

4.3 Comparison to state-of-the-art

Our best model uses the proposed space-time mixing attention in all the Transformer layers and performs temporal aggregation using a single lightweight temporal transformer layer as described in Section 3. Unless otherwise specified, we report the results using the 1×3 configuration for the views (1 temporal and 3 spatial) for all datasets.

On **Kinetics-400**, we match the current state-of-the-art results while being significantly faster than the next two best recently/concurrently proposed methods that also use Transformer-based architectures:

Table 6: Comparison with state-of-the-art on SSv2. $T\times$ is the number of frames used by our method.

Method	Top-1	Top-5	Views	FLOPs ($\times 10^9$)
TRN [49]	48.8	77.6	-	-
SlowFast+multigrid [43]	61.7	-	1×3	-
TimeSformer-L [3]	62.4	-	1×3	7,140
TSM R50 [25]	63.3	88.5	2×3	-
STM [18]	64.2	89.8	-	-
MSNet [23]	64.7	89.4	-	-
TEA [24]	65.1	-	-	-
ViViT-L/16x2 [3]	**65.4**	89.8	4×3	11,892
X-ViT (8$\times$) (Ours)	63.4	89.6	1×3	425
X-ViT (16$\times$) (Ours)	65.2	90.6	1×3	850
X-ViT (32$\times$) (Ours)	**65.4**	**90.7**	1×3	1,270

$20\times$ faster than ViVit [1] and $8\times$ than TimeSformer-L [3]. Note that both the models from [1, 3] and ours were initialized from a ViT model pretrained on ImageNet-21k [10] and take as input frames at a resolution of 224×224px. See the supplementary material for results on Kinetics-600.

On **SSv2** we match and surpass the current state-of-the-art, especially in terms of Top-5 accuracy (ours: 90.7% vs ViViT: 89.8% [1]) using models that are $14\times$ (16 frames) and $9\times$ (32 frames) faster.

Finally, we observe similar outcomes on the **Epic-100** where we set a new state-of-the-art, showing particularly large improvements especially for "Verb" accuracy, while again being more efficient.

5 Ethical considerations and broader impact

Current high-performing video recognition models tend to have high computational demands for both training and testing and, by extension, significant environmental costs. This is especially true of the transformer architectures. Our research introduces a novel approach that matches and surpasses the current state-of-the-art while being significantly more efficient thanks to the linear scaling of the complexity with respect to the number of frames. We hope such models will offer noticeable reduction in power consumption while setting at the same time a solid base for future research. We will release code and models to facilitate this. Moreover, and similarly to most data-driven systems, bias from the training data can potentially affect the fairness of the model. As such, we suggest to take this aspect into consideration when deploying the models into real-world scenarios.

Table 7: Comparison with state-of-the-art on Epic-100. $T\times$ is the #frames used by our method. Results for other methods are taken from [1].

Method	Action	Verb	Noun
TSN [39]	33.2	60.2	46.0
TRN [49]	35.3	65.9	45.4
TBN [21]	36.7	66.0	47.2
TSM [21]	38.3	67.9	49.0
SlowFast [15]	38.5	65.6	50.0
ViViT-L/16x2 [1]	44.0	66.4	**56.8**
X-ViT (8$\times$) (Ours)	41.5	66.7	53.3
X-ViT (16$\times$) (Ours)	**44.3**	**68.7**	56.4

6 Conclusions

We presented a novel approximation to the full space-time attention that is amenable to an efficient implementation and applied it to video recognition. Our approximation has the same computational cost as spatial-only attention yet the resulting Video Transformer model was shown to be significantly more efficient than recently/concurrently proposed Video Transformers [3, 1]. By no means this paper proposes a complete solution to video recognition using Video Transformers. Future efforts could include combining our approaches with other architectures than the standard ViT, removing the dependency on pre-trained models and applying the model to other video-related tasks like detection and segmentation. Finally, further research is required for deploying our models on low power devices.

References

[1] Anurag Arnab, Mostafa Dehghani, Georg Heigold, Chen Sun, Mario Lučić, and Cordelia Schmid. Vivit: A video vision transformer. *arXiv preprint arXiv:2103.15691*, 2021.

[2] Iz Beltagy, Matthew E Peters, and Arman Cohan. Longformer: The long-document transformer. *arXiv preprint arXiv:2004.05150*, 2020.

[3] Gedas Bertasius, Heng Wang, and Lorenzo Torresani. Is space-time attention all you need for video understanding? *arXiv preprint arXiv:2102.05095*, 2021.

[4] Joao Carreira and Andrew Zisserman. Quo vadis, action recognition? a new model and the kinetics dataset. In *proceedings of the IEEE Conference on Computer Vision and Pattern Recognition*, pages 6299–6308, 2017.

[5] Mia Xu Chen, Orhan Firat, Ankur Bapna, Melvin Johnson, Wolfgang Macherey, George Foster, Llion Jones, Niki Parmar, Mike Schuster, Zhifeng Chen, et al. The best of both worlds: Combining recent advances in neural machine translation. *arXiv preprint arXiv:1804.09849*, 2018.

[6] Yunpeng Chen, Yannis Kalantidis, Jianshu Li, Shuicheng Yan, and Jiashi Feng. A2-nets: Double attention networks. *arXiv preprint arXiv:1810.11579*, 2018.

[7] Ekin D Cubuk, Barret Zoph, Dandelion Mane, Vijay Vasudevan, and Quoc V Le. Autoaugment: Learning augmentation policies from data. *arXiv preprint arXiv:1805.09501*, 2018.

[8] Dima Damen, Hazel Doughty, Giovanni Maria Farinella, Sanja Fidler, Antonino Furnari, Evangelos Kazakos, Davide Moltisanti, Jonathan Munro, Toby Perrett, Will Price, et al. Scaling egocentric vision: The epic-kitchens dataset. In *ECCV*, 2018.

[9] Dima Damen, Hazel Doughty, Giovanni Maria Farinella, Antonino Furnari, Evangelos Kazakos, Jian Ma, Davide Moltisanti, Jonathan Munro, Toby Perrett, Will Price, et al. Rescaling egocentric vision. *arXiv preprint arXiv:2006.13256*, 2020.

[10] Jia Deng, Wei Dong, Richard Socher, Li-Jia Li, Kai Li, and Li Fei-Fei. Imagenet: A large-scale hierarchical image database. In *2009 IEEE conference on computer vision and pattern recognition*, pages 248–255. Ieee, 2009.

[11] Jacob Devlin, Ming-Wei Chang, Kenton Lee, and Kristina Toutanova. Bert: Pre-training of deep bidirectional transformers for language understanding. *arXiv preprint arXiv:1810.04805*, 2018.

[12] Alexey Dosovitskiy, Lucas Beyer, Alexander Kolesnikov, Dirk Weissenborn, Xiaohua Zhai, Thomas Unterthiner, Mostafa Dehghani, Matthias Minderer, Georg Heigold, Sylvain Gelly, et al. An image is worth 16x16 words: Transformers for image recognition at scale. *arXiv preprint arXiv:2010.11929*, 2020.

[13] Quanfu Fan, Chun-Fu Chen, Hilde Kuehne, Marco Pistoia, and David Cox. More is less: Learning efficient video representations by big-little network and depthwise temporal aggregation. *arXiv preprint arXiv:1912.00869*, 2019.

[14] Christoph Feichtenhofer. X3d: Expanding architectures for efficient video recognition. In *Proceedings of the IEEE/CVF Conference on Computer Vision and Pattern Recognition*, pages 203–213, 2020.

[15] Christoph Feichtenhofer, Haoqi Fan, Jitendra Malik, and Kaiming He. Slowfast networks for video recognition. In *Proceedings of the IEEE/CVF International Conference on Computer Vision*, pages 6202–6211, 2019.

[16] Raghav Goyal, Samira Ebrahimi Kahou, Vincent Michalski, Joanna Materzynska, Susanne Westphal, Heuna Kim, Valentin Haenel, Ingo Fruend, Peter Yianilos, Moritz Mueller-Freitag, et al. The" something something" video database for learning and evaluating visual common sense. In *Proceedings of the IEEE International Conference on Computer Vision*, pages 5842–5850, 2017.

[17] Kaiming He, Xiangyu Zhang, Shaoqing Ren, and Jian Sun. Deep residual learning for image recognition. In *Proceedings of the IEEE conference on computer vision and pattern recognition*, pages 770–778, 2016.

[18] Boyuan Jiang, MengMeng Wang, Weihao Gan, Wei Wu, and Junjie Yan. Stm: Spatiotemporal and motion encoding for action recognition. In *Proceedings of the IEEE/CVF International Conference on Computer Vision*, pages 2000–2009, 2019.

[19] Andrej Karpathy, George Toderici, Sanketh Shetty, Thomas Leung, Rahul Sukthankar, and Li Fei-Fei. Large-scale video classification with convolutional neural networks. In *Proceedings of the IEEE conference on Computer Vision and Pattern Recognition*, pages 1725–1732, 2014.

[20] Will Kay, Joao Carreira, Karen Simonyan, Brian Zhang, Chloe Hillier, Sudheendra Vijayanarasimhan, Fabio Viola, Tim Green, Trevor Back, Paul Natsev, et al. The kinetics human action video dataset. *arXiv preprint arXiv:1705.06950*, 2017.

[21] Evangelos Kazakos, Arsha Nagrani, Andrew Zisserman, and Dima Damen. Epic-fusion: Audio-visual temporal binding for egocentric action recognition. In *Proceedings of the IEEE/CVF International Conference on Computer Vision*, pages 5492–5501, 2019.

[22] Alex Krizhevsky, Ilya Sutskever, and Geoffrey E Hinton. Imagenet classification with deep convolutional neural networks. *Advances in neural information processing systems*, 25:1097–1105, 2012.

[23] Heeseung Kwon, Manjin Kim, Suha Kwak, and Minsu Cho. Motionsqueeze: Neural motion feature learning for video understanding. In *European Conference on Computer Vision*, pages 345–362. Springer, 2020.

[24] Yan Li, Bin Ji, Xintian Shi, Jianguo Zhang, Bin Kang, and Limin Wang. Tea: Temporal excitation and aggregation for action recognition. In *Proceedings of the IEEE/CVF Conference on Computer Vision and Pattern Recognition*, pages 909–918, 2020.

[25] Ji Lin, Chuang Gan, and Song Han. Tsm: Temporal shift module for efficient video understanding. In *Proceedings of the IEEE/CVF International Conference on Computer Vision*, pages 7083–7093, 2019.

[26] Zhaoyang Liu, Limin Wang, Wayne Wu, Chen Qian, and Tong Lu. Tam: Temporal adaptive module for video recognition. *arXiv preprint arXiv:2005.06803*, 2020.

[27] Ilya Loshchilov and Frank Hutter. Sgdr: Stochastic gradient descent with warm restarts. *arXiv preprint arXiv:1608.03983*, 2016.

[28] Adam Paszke, Sam Gross, Francisco Massa, Adam Lerer, James Bradbury, Gregory Chanan, Trevor Killeen, Zeming Lin, Natalia Gimelshein, Luca Antiga, et al. Pytorch: An imperative style, high-performance deep learning library. *arXiv preprint arXiv:1912.01703*, 2019.

[29] Zhaofan Qiu, Ting Yao, Chong-Wah Ngo, Xinmei Tian, and Tao Mei. Learning spatio-temporal representation with local and global diffusion. In *Proceedings of the IEEE/CVF Conference on Computer Vision and Pattern Recognition*, pages 12056–12065, 2019.

[30] Colin Raffel, Noam Shazeer, Adam Roberts, Katherine Lee, Sharan Narang, Michael Matena, Yanqi Zhou, Wei Li, and Peter J Liu. Exploring the limits of transfer learning with a unified text-to-text transformer. *arXiv preprint arXiv:1910.10683*, 2019.

[31] Aravind Srinivas, Tsung-Yi Lin, Niki Parmar, Jonathon Shlens, Pieter Abbeel, and Ashish Vaswani. Bottleneck transformers for visual recognition. *arXiv preprint arXiv:2101.11605*, 2021.

[32] Christian Szegedy, Vincent Vanhoucke, Sergey Ioffe, Jon Shlens, and Zbigniew Wojna. Rethinking the inception architecture for computer vision. In *Proceedings of the IEEE conference on computer vision and pattern recognition*, pages 2818–2826, 2016.

[33] Hugo Touvron, Matthieu Cord, Matthijs Douze, Francisco Massa, Alexandre Sablayrolles, and Hervé Jégou. Training data-efficient image transformers & distillation through attention. *arXiv preprint arXiv:2012.12877*, 2020.

[34] Du Tran, Lubomir Bourdev, Rob Fergus, Lorenzo Torresani, and Manohar Paluri. Learning spatiotemporal features with 3d convolutional networks. In *Proceedings of the IEEE international conference on computer vision*, pages 4489–4497, 2015.

[35] Du Tran, Heng Wang, Lorenzo Torresani, Jamie Ray, Yann LeCun, and Manohar Paluri. A closer look at spatiotemporal convolutions for action recognition. In *Proceedings of the IEEE conference on Computer Vision and Pattern Recognition*, pages 6450–6459, 2018.

[36] Du Tran, Heng Wang, Lorenzo Torresani, and Matt Feiszli. Video classification with channel-separated convolutional networks. In *Proceedings of the IEEE/CVF International Conference on Computer Vision*, pages 5552–5561, 2019.

[37] Ashish Vaswani, Noam Shazeer, Niki Parmar, Jakob Uszkoreit, Llion Jones, Aidan N Gomez, Lukasz Kaiser, and Illia Polosukhin. Attention is all you need. *arXiv preprint arXiv:1706.03762*, 2017.

[38] Heng Wang, Du Tran, Lorenzo Torresani, and Matt Feiszli. Video modeling with correlation networks. In *Proceedings of the IEEE/CVF Conference on Computer Vision and Pattern Recognition*, pages 352–361, 2020.

[39] Limin Wang, Yuanjun Xiong, Zhe Wang, Yu Qiao, Dahua Lin, Xiaoou Tang, and Luc Van Gool. Temporal segment networks: Towards good practices for deep action recognition. In *European conference on computer vision*, pages 20–36. Springer, 2016.

[40] Limin Wang, Yuanjun Xiong, Zhe Wang, Yu Qiao, Dahua Lin, Xiaoou Tang, and Luc Van Gool. Temporal segment networks for action recognition in videos. *IEEE transactions on pattern analysis and machine intelligence*, 41(11):2740–2755, 2018.

[41] Xiaolong Wang, Ross Girshick, Abhinav Gupta, and Kaiming He. Non-local neural networks. In *Proceedings of the IEEE conference on computer vision and pattern recognition*, pages 7794–7803, 2018.

[42] Bichen Wu, Alvin Wan, Xiangyu Yue, Peter Jin, Sicheng Zhao, Noah Golmant, Amir Gholaminejad, Joseph Gonzalez, and Kurt Keutzer. Shift: A zero flop, zero parameter alternative to spatial convolutions. In *CVPR*, 2018.

[43] Chao-Yuan Wu, Ross Girshick, Kaiming He, Christoph Feichtenhofer, and Philipp Krahenbuhl. A multigrid method for efficiently training video models. In *Proceedings of the IEEE/CVF Conference on Computer Vision and Pattern Recognition*, pages 153–162, 2020.

[44] Saining Xie, Ross Girshick, Piotr Dollár, Zhuowen Tu, and Kaiming He. Aggregated residual transformations for deep neural networks. In *Proceedings of the IEEE conference on computer vision and pattern recognition*, pages 1492–1500, 2017.

[45] Li Yuan, Yunpeng Chen, Tao Wang, Weihao Yu, Yujun Shi, Francis EH Tay, Jiashi Feng, and Shuicheng Yan. Tokens-to-token vit: Training vision transformers from scratch on imagenet. *arXiv preprint arXiv:2101.11986*, 2021.

[46] Han Zhang, Ian Goodfellow, Dimitris Metaxas, and Augustus Odena. Self-attention generative adversarial networks. In *International conference on machine learning*, pages 7354–7363. PMLR, 2019.

[47] Hongyi Zhang, Moustapha Cisse, Yann N Dauphin, and David Lopez-Paz. mixup: Beyond empirical risk minimization. *arXiv preprint arXiv:1710.09412*, 2017.

[48] Zhun Zhong, Liang Zheng, Guoliang Kang, Shaozi Li, and Yi Yang. Random erasing data augmentation. In *Proceedings of the AAAI Conference on Artificial Intelligence*, volume 34, pages 13001–13008, 2020.

[49] Bolei Zhou, Alex Andonian, Aude Oliva, and Antonio Torralba. Temporal relational reasoning in videos. In *Proceedings of the European Conference on Computer Vision (ECCV)*, pages 803–818, 2018.

Checklist

1. For all authors...
   (a) Do the main claims made in the abstract and introduction accurately reflect the paper's contributions and scope? [Yes]
   (b) Did you describe the limitations of your work? [Yes] See Section 6
   (c) Did you discuss any potential negative societal impacts of your work? [Yes] See Section 5
   (d) Have you read the ethics review guidelines and ensured that your paper conforms to them? [Yes]
2. If you are including theoretical results...
   (a) Did you state the full set of assumptions of all theoretical results? [N/A]
   (b) Did you include complete proofs of all theoretical results? [N/A]
3. If you ran experiments...
   (a) Did you include the code, data, and instructions needed to reproduce the main experimental results (either in the supplemental material or as a URL)? [No] We include however all implementation details required to reproduce our work. We will make the code and the models available. The datasets used are already publicly available.
   (b) Did you specify all the training details (e.g., data splits, hyperparameters, how they were chosen)? [Yes] See Section 4.1

(c) Did you report error bars (e.g., with respect to the random seed after running experiments multiple times)? [Yes] Due to prohibitive costs, we reported the variations between multiple training runs for a single 8 frames model in Section 4.1. This should be representative for the rest of the trained models.

(d) Did you include the total amount of compute and the type of resources used (e.g., type of GPUs, internal cluster, or cloud provider)? [Yes] See Section 4.1

4. If you are using existing assets (e.g., code, data, models) or curating/releasing new assets...

(a) If your work uses existing assets, did you cite the creators? [Yes]

(b) Did you mention the license of the assets? [Yes] See Section 4.1

(c) Did you include any new assets either in the supplemental material or as a URL? [N/A]

(d) Did you discuss whether and how consent was obtained from people whose data you're using/curating? [N/A] No data was collected, publicly available datasets were used

(e) Did you discuss whether the data you are using/curating contains personally identifiable information or offensive content? [Yes] To our knowledge the datasets used do not contain such info

5. If you used crowdsourcing or conducted research with human subjects...

(a) Did you include the full text of instructions given to participants and screenshots, if applicable? [N/A]

(b) Did you describe any potential participant risks, with links to Institutional Review Board (IRB) approvals, if applicable? [N/A]

(c) Did you include the estimated hourly wage paid to participants and the total amount spent on participant compensation? [N/A]